Transactions of the Korean Nuclear Society Spring Meeting
Jeju, Korea, May 17-18, 2018

Benchmarking of the four-sensor optical fiber probe method for the measurement of local bubble parameters under the slug flow

Jeongmin Moon, Taeho Kim, Jaejun Jeong, Byongjo Yun*
School of Mechanical Engineering, Pusan Nat'l Univ., Jangjeon2-dong, Geumjeong-gu, Busan, Korea
**Corresponding author: bjyun@pusan.ac.kr*

1. Introduction

Bubble parameters such as void fraction, bubble velocity, and interfacial area concentration (IAC) are important for an accurate prediction of bubble behaviors in the two-phase flow. For the past decades, a number of researches have applied multiple sensor probe method to measure local bubble parameters [1-7]. The four-sensor probe method is one of the representative multi-sensor probe methods which can measure the local bubble parameters regardless of bubble shape and bubble behavior [1, 3-6]. However, there is a lack of evaluation as to whether it is applicable to flow conditions in which distorted and slug bubbles appear.

In the present study, the performance of four-sensor probe was investigated with numerical simulations under the postulated flow conditions for various bubble shapes simulating slug bubble. Also, In order to quantitatively evaluate the performance of the four-sensor optical fiber probe (4S-OFP) under actual flow conditions, a verification experiment was carried out by applying both a visualization technique and a four-sensor probe method to the rectangular channel under the air-water flow condition.

2. Four-sensor optical fiber probe method

The optical fiber sensor distinguishes phases by using the intensity of the laser back-scattered due to the refractive index difference of the interface at the two-phase flow. The design of the four-sensor optical fiber probe (4S-OFP) is shown in Fig. 1(Left). As you can see in Fig. 1(Left), 4S-OFP consists of one front sensor and three rear sensors located on the same plane. Fig. 1(Right) shows a typical signal of the bubble measured by the 4S-OFP. Local bubble parameters such as the void fraction, bubble velocity, and interface area concentration (IAC) can be calculated using time intervals (τ_b, Δt) measured from the sensor signal in Fig. 1(Right).

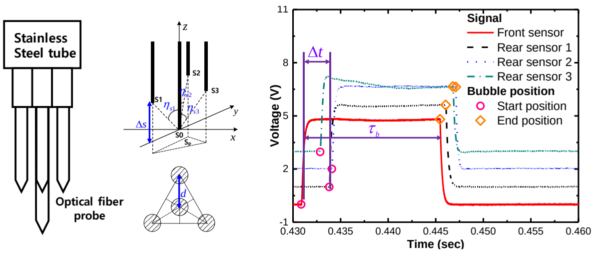

Fig. 1. The four-sensor optical fiber probe
(Left: Design of 4S-OFP, Right: Typical bubble signal)

The local void fraction (α) is calculated as the ratio of the bubble passing time (τ_b) to the measured time (Ω) as follows.

$$\alpha = \frac{\sum_{j=1}^{N_b} (\tau_b)_j}{\Omega} \tag{1}$$

The bubble velocity ($v_{4S\text{-}OFP}$) is calculated using three pairs of double-sensor combined front sensor with rear sensor as shown in Eq. (2) [8].

$$\left|v_{4S\text{-}OFP}\right|^2 = \frac{|A_0|}{\sqrt{A_1^2 + A_2^2 + A_3^2}},\ A = f(v, \eta) \tag{2}$$

The IAC is one of the main parameters for determining the mass, momentum and energy transfer between phases, which is defined as a function of bubble velocity by a number of researchers. Existing IAC measurement method are summarized in Table 1.

Table 1. Existing IAC measurement methods

Researcher	IAC measurement method
Kataoka et al. [1]	$a_i = \frac{1}{\Omega}\left\{\left(\frac{1}{v_{s1j}}\right)^2 + \left(\frac{1}{v_{s2j}}\right)^2 + \left(\frac{1}{v_{s3j}}\right)^2\right\}$
Revankar et al. [3]	$a_i = \frac{1}{\Omega}\left\{\left(\frac{1}{v_{s1j}}\right)^2 + \left(\frac{1}{v_{s2j}}\right)^2 + \left(\frac{1}{v_{s3j}}\right)^2\right\} + \frac{\tau_{b,\text{missing}}}{\Omega}\frac{l_b}{s_p}$
Le Corre et al. [9]	$a_i = \frac{1}{\Omega\sqrt{1-\sqrt{2.4 r_N - 1.5 r_N^2}}}\left\{\left(\frac{1}{v_{s1j}}\right)^2 + \left(\frac{1}{v_{s2j}}\right)^2 + \left(\frac{1}{v_{s3j}}\right)^2\right\}$

3. Numerical simulation for performance evaluation of 4S-OFP

3.1 Monte carlo simulation

The bubble parameters using the 4S-OFP are affected by the missing signal which occur when bubbles do not pass through all of the sensors. Therefore, in order to derive the optimized geometry of probe that minimizes the influence of the missing signal, factors affecting the measurement should be comprehensively evaluated.

In this chapter, the performance of 4S-OFP was evaluated in various bubble flow conditions using Monte Carlo simulation. Simulation was performed considering the flow condition of the bubble, the bubble shape with various aspect ratios, and the geometrical configuration of the 4S-OFP. Fig. 2 shows the flow chart of simulation.

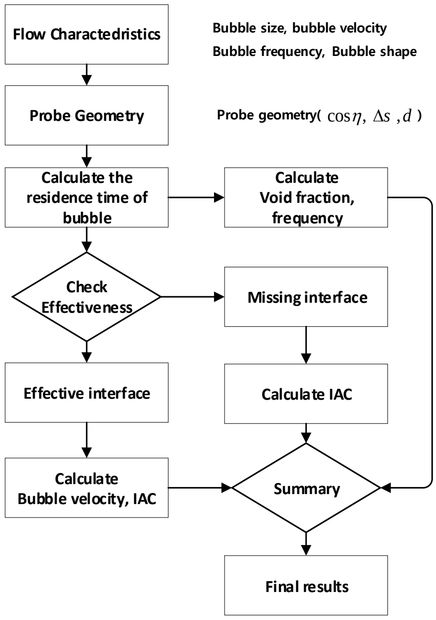

Fig. 2. Flow chart for Monte Carlo simulation

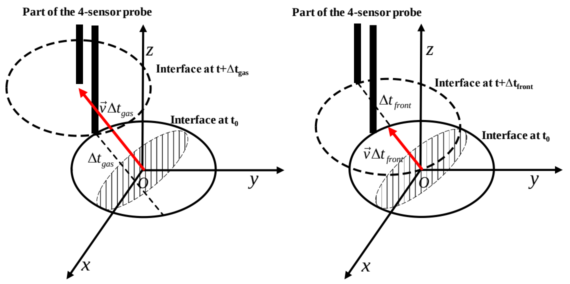

Fig. 3. Diagram of a bubble passing sensors of the probe

In order to calculate void fraction, bubble velocity and IAC at the local point through the simulation, it is necessary to define the time intervals *(Δt_{gas} , $\Delta t_{front\ or\ rear}$)* as shown in Fig. 3. It can be obtained by using the equation of the bubble interface that is formulated according to time as shown in Eq. (3).

$$\left(x_k - v_x \Delta t\right)^2 + \left(y_k - v_y \Delta t\right)^2 + \frac{\left(z_k - v_z \Delta t\right)^2}{\beta} = R^2 \qquad (3)$$

Where (x_k, y_k, z_k) represents the position of the sensor in contact with the bubble interface, which is defined by dividing the front sensor (*k=0*) and rear sensor (*k=1, 2, 3*) using subscripts. The probability distribution of the position is uniform in the bubble cross-sectional area to the bubble velocity direction (the shaded area) in Fig. 3.

The bubble motion swing to the left and right due to the turbulent flow was simulated using the relative turbulent intensity (H) as shown in Eq. (4) which was first used by Wu et al [10]. The geometrical design parameters of the 4S-OFP were evaluated according to the radial distance (d) and the vertical distance (Δs) as shown in Fig 1.

$$\vec{v} = \bar{v}\vec{k} + \vec{v}\,' = \bar{v}\left(\vec{k} + H\vec{n}_v\right) \qquad (4)$$

3.2 Simulation results

The measurement performance of 4S-OFP was evaluated through Monte Carlo simulation. The simulation was performed considering various flow conditions, various bubble shapes, and the geometry of the 4S-OFP. As a result of simulation, the accuracy of bubble velocity measurement is better as the radial distance between sensors is closer. On the other hand, the vertical distance between the sensors did not affect the velocity measurement. The accuracy of IAC measurement was most excellent in IAC measurement method proposed by Revankar et al. [3] In case of the 4S-OFP geometry effect on the IAC, it is negligible in slug bubble with large aspect ratio. As the turbulent intensity increases, the accuracy of measuring the IAC decreases. However, turbulent intensity does not affect significantly the measurement of the 4-sensor probe because the bubbles cover the cross section of the channel under the slug flow.

By these numerical simulations, it is possible to determine the optimal geometry of the probe under a given flow condition. However, this numerical simulation has limitations because it does not consider the actual behavior of bubbles in the flow channel. Therefore, we performed a verification experiment in the rectangular channel under the air-water flow condition.

4. Verification experiment for 4S-OFP performance

4.1 Experimental apparatus

Fig. 5(Left) is a schematic diagram of an experimental apparatus for verifying the performance of an in-house developed 4S-OFP. The experimental apparatus consisted of an air-water flowing test section and a bubble generator. The test section is designed as a rectangular channel with a cross section of 20 mm x 20 mm and 1 m in length.

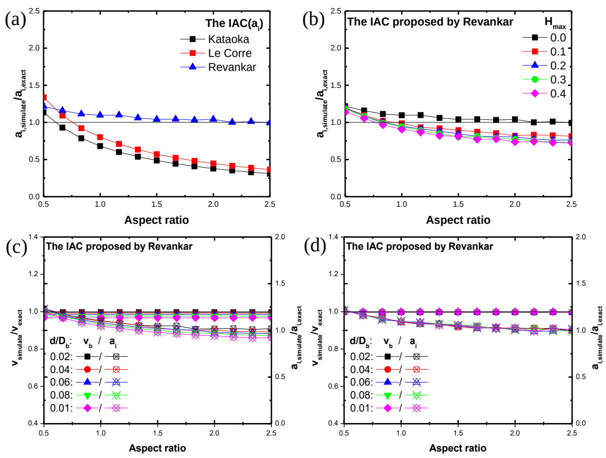

Fig. 4. The simulation results
(a: IAC measurement method, b: Turbulent effect, c, d :4S-OFP geometry effect)

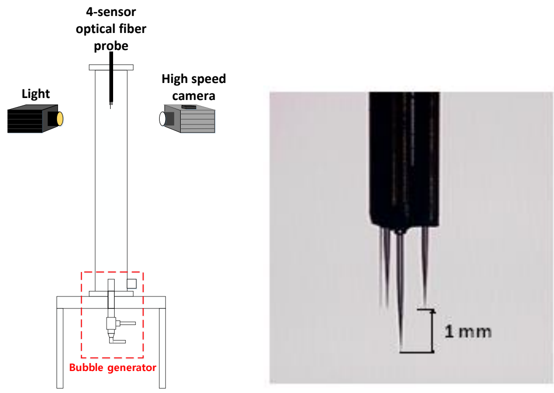

Fig. 5. Experimental facility
(Left: Schematic diagram, Right: In-house 4S-OFP)

The bubble generator is located at the bottom of the test section. Bubbles are generated by varying the injection rate of water and air to control the size of bubbles. The 4S-OFP (Fig. 5(Right)) was installed at position 0.8 m (L/D = 40) from the entrance. Also, the high-speed camera was applied at the same height of test section. From the test, we compared the data from visualization with the data from the 4S-OFP.

4.2 Visualization method

The local bubble parameters are obtained by image processing as shown in Fig. 6. As the first step of the image processing, auto-binarization method was applied to the raw image (Fig. 6(a)) to identify the bubble boundary. However, since there is a possibility that the boundary of the bubble is not distinguished due to the light reflection, the morphology operation was applied to distinguish bubble boundary clearly. Fig. 6(c) shows the final result of applying the image processing.

The local void fraction is obtained from the bubble image with image processing. The local bubble velocity is also calculated by using the movement distance according to the change of frame interval. The IAC is calculated using Eq. (5) and the upper boundary of the bubble, which is expressed by the 6th order polynomial function [11].

$$a_i(r) = \left(1 + \sqrt{\frac{df(r)}{dr} + 1}\right) \frac{N_s}{v_s} \tag{5}$$

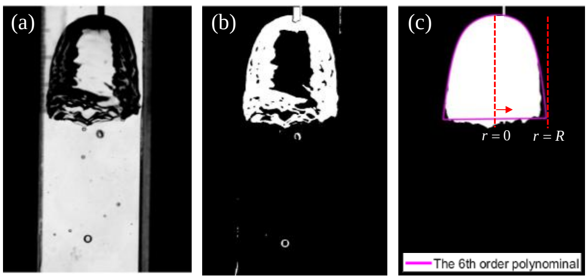

Fig. 6. Procedure for image processing
(a : Raw image, b: Binary image, c: Final bubble image)

Where *f(r)* is function for the upper boundary of the bubble derived by the least squares method. N_s is the number of slug bubbles passing through the sensor per unit time. v_s is the velocity of the slug bubble.

4.3 Experimental results

In cap-bubbly flow or slug flow conditions, The experimental results measured by the visualization and the 4S-OFP were compared. Fig.7 shows experimental results depending on the aspect ratio of the bubbles. As shown in Fig. 7(a), the 4S-OFP can measure the void fraction within the error 10%. Additionally, the bubble velocity and IAC were measured within error of 8% and 22%, respectively. The measurement error of IAC is mainly resulted by asymmetric shape of bubbles.

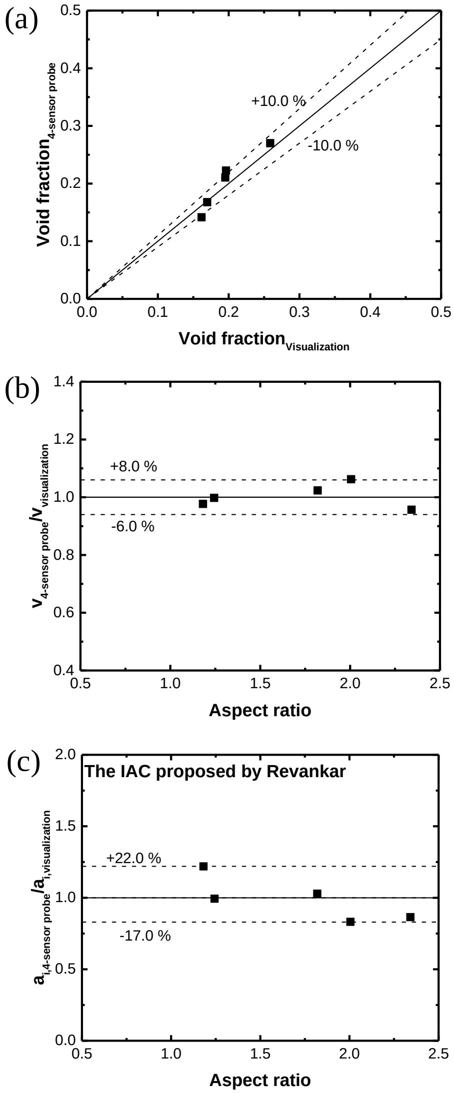

Fig. 7. Experimental results
(a: Void fraction, b: Bubble velocity, c: IAC)

5. Conclusion

In this study, Monte Carlo simulation and verification experiments were conducted to develop the 4-sensor optical fiber probe (4S-OFP) methodology for bubble parameters. In the simulation, the optimized geometry of probe could be designed by evaluating the 4S-OFP performance according to the sensor design parameters. Simulation results show that the bubble velocity was measured more accurately as the radial distance between the sensors was closer. On the other hand, the influence of the vertical distance between sensors was insignificant. In case of the interfacial area concentration (IAC), the IAC methodology proposed by Revankar et al. [3] showed the best accuracy. The influence of the probe geometry on the IAC measurement performance was not significant. However, due to the coexistence of various shapes of bubble, the actual bubbly flow requires a comprehensive evaluation of the bubble. Therefore, the performance of 4S-OFP was evaluated through the verification experiment in the square channel under the air-water flow condition. Experiments were carried out under cap-bubbly flow and slug flow conditions. The measured parameters are the local parameters including the void fraction, the bubble velocity, and the IAC. The performance of the 4S-OFP was evaluated by comparing the bubble parameters measured with the visualization. As a result, 4S-OFP was measured within 10%, 8%, and 22% error of void fraction, bubble velocity and IAC, respectively, in the cap-bubbly or slug flow conditions.

Acknowledgement

This work was supported by the Nuclear Safety Research Program through the Korea Foundation Of Nuclear Safety (KoFONS) using the financial resource granted by the Nuclear Safety and Security Commission (NSSC) of the Republic of Korea. (No. 1305011) and the Nuclear Research & Development Program of the NRF (National Research Foundation of Korea) grant funded by the MSIT (Ministry of Science, ICT), Republic of Korea (No. NRF-2017M2A8A4015059).

REFERENCES

[1] I. Kataoka, M. Ishii, and A. Serizawa, Local formulation and measurements of interfacial area concentration in two-phase flow, International Journal of Multiphase Flow, Vol.12, p. 505, 1986.
[2] T. Hibiki, S. Hogsett, and M. Ishii, Local measurement of interfacial area, interfacial velocity and liquid turbulence in two-phase flow, Nuclear Engineering and Design, Vol.184, p. 287, 1998.
[3] S. T. Revankar, and M. Ishii, Theory and measurement of local interfacial area using a four sensor probe in two-phase flow, International journal of heat and mass transfer, Vol.36, p. 2997, 1993.
[4] J. M. Burgess, and P. H. Calderbank, The measurement of bubble parameters in two-phase dispersions I: the development of an improved probe technique, Chemical engineering science, Vol.30, p. 743, 1975.
[5] M. Higuchi, and T. Saito, Quantitative characterizations of long-period fluctuations in a large-diameter bubble column based on point-wise void fraction measurements, Chemical Engineering Journal, Vol.160, p. 284, 2010.
[6] X. Shen, and H. Nakamura, Local interfacial velocity measurement method using a four-sensor probe, International journal of heat and mass transfer, Vol.67, p. 843, 2013.
[7] T. Worosz, M. Bernard, R. Kong, A. Toptan, S. Kim, and C. Hoxie, Sensitivity studies on the multi-sensor conductivity probe measurement technique for two-phase flows, Nuclear Engineering and Design, Vol.310, p. 552, 2016.
[8] D. J. Euh, B. J. Yun, and C. H. Song, Numerical simulation of an improved five-sensor probe method for local interfacial area concentration measurement, Nuclear engineering and design, Vol.234, p. 99, 2004.
[9] J. M. Le Corre, and M. Ishii, Numerical evaluation and correction method for multi-sensor probe measurement techniques in two-phase bubbly flow, Nuclear engineering and design, Vol.216, p 221, 2002.
[10] Q. Wu, and M. Ishii, Sensitivity study on double-sensor conductivity probe for the measurement of interfacial area concentration in bubbly flow, International Journal of Multiphase Flow, Vol.25, p. 155, 1999.
[11] S. Kim, X. Y. Fu, X. Wang, and M. Ishii, Study on interfacial structures in slug flows using a miniaturized four-sensor conductivity probe. Nuclear engineering and design, Vol.204, p. 45, 2001.